JOURNAL OF RESEARCH of the National Bureau of Standards—D. Radio Propagation
Vol. 65D, No. 2, March–April 1961

Ionospheric Motions Observed with High Frequency Backscatter Sounders[1]

Lowell H. Tveten

(November 3, 1960)

Techniques for determining the characteristics of movements of irregularities in the $F2$-region by the use of backscatter records are described. The results of an analysis of backscatter data obtained during December 1952, at Sterling, Virginia, at a frequency of about 13.7 Mc/s are presented and found to be in good agreement with those of other investigators of ionospheric motions.

1. Introduction

Winds and apparent motions in the ionosphere have been the subjects of study by various groups for some time. Different methods have been used. Included among the radio techniques are radio fading patterns [Mitra, 1949; Salzberg and Greenstone, 1951; Chapman, 1953], spaced vertical sounders [Munro, 1948; Munro, 1950; Price, 1954], direction-of-arrival studies [Bramley and Ross, 1951] and others [Meek, 1949; Gerson, 1950; Manning, Villard, and Peterson, 1950; Maxwell and Little, 1952; Maxwell and Dagg, 1954; Maxwell 1954; Clark and Peterson, 1956; McNicol and Webster, 1956; Wells, 1957; Valverde, 1958]. It is the purpose of this paper to present another method for studying ionospheric motions and give some results and conclusions obtained using this method.

Use of backscatter sounding was made at Stanford University to study motions of sporadic-E clouds [Clark and Peterson, 1956] and very large disturbances in the $F2$-layer [Valverde, 1958]. The present paper also deals with $F2$-layer disturbances, some of which appear to be like those studied by Valverde [1958] although the technique of analysis used is different. For the most part, however, the paper deals with disturbances of a smaller size and the technique of determining the motion is new. Some preliminary results of this investigation were mentioned by Wells [1957].

2. General Background and Method

2.1. Backscatter Sounding and Recording Techniques

For those unfamiliar with backscatter sounding a brief explanation is in order. A pulse of radio frequency energy is radiated from a directive antenna. This pulse travels outward until it encounters the ionospheric layers at one of which it may be reflected back down to earth. At the ground the energy is reflected and scattered in all directions. Some of the scattered energy retraces its original path and arrives back at the transmitting point at a delay time equal to the length of the path traveled by the pulse divided by the appropriate average group velocity of the wave over the path. This scattered energy is then channeled through a radio pulse receiver whose output is recorded.

For the purpose of this experiment the radiating antenna should not have appreciable directivity in the vertical plane but should be fairly directive in the horizontal plane. Under these conditions backscatter energy is obtained from the edge of the "skip zone" for the particular frequency and ionospheric layer involved and on to greater ranges with general decrease in intensity as the range increases [Hartsfield, Ostrow, and Silberstein, 1950; Dieminger, 1951; Peterson, 1951; Hartsfield and Silberstein, 1952; Silberstein, 1953; Shearman, 1956].

One of the methods of recording backscatter is the "range-time" recording technique in which an oscilloscope trace is triggered at the same time as the transmitter pulse, and the backscatter signal from the receiver is used to intensity modulate the trace. This trace is then photographed by a moving film camera in which the image of the trace on the film is perpendicular to the direction of film travel. The result is a plot of backscatter range as a function of time. Another method is the plan position indicator (PPI) display in which an intensity modulated oscilloscope trace rotates in synchronism with a rotating directive antenna. A photograph of one complete rotation then displays the scatter characteristics as a function of azimuth.

The range-time sweep may be gated to display only a certain portion of the total range. This is done to display greater detail of backscatter signal. An example of this type of record is shown in figure 1. The delay time is given in milliseconds and represents twice the slant range to the ground scattering point divided by the speed of propagation. The time base is in hours. For this particular record a pulse length of about 70 μsec was used and the antenna was a large terminated rhombic.

The record shows that backscatter has a quite complicated structure as far as amplitude versus range is concerned. The immediately striking feature of the record is that the amplitude peaks tend to

[1] Contribution from Central Radio Propagation Laboratory, National Bureau of Standards, Boulder, Colo.

574930—61——1

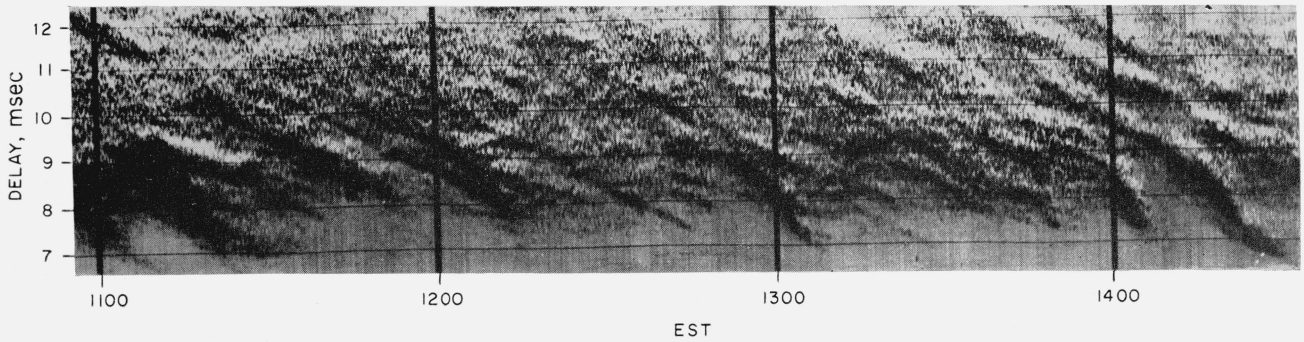

FIGURE 1. *Backscatter record made at Sterling, Virginia on 13.7 Mc/s at azimuth 282°, November 9, 1955.*

maintain themselves over relatively long periods of time but change in range during that time. This is the feature which is taken as evidence of ionospheric motions and the characteristics of these "ripples" in the backscatter are used to interpret the nature of the motions.

2.2. Quantitative Basis for Deduction of Motion Characteristics From Backscatter Records

A focusing phenomenon is necessary for the formation of amplitude peaks. Where along the path followed by the pulse does the focusing occur? Focusing regions below the ionospheric reflection point should be equally effective whether they occur on the near side or far side of the ionospheric reflection point with respect to the transmitter. However, the magnitude of the apparent motion of the focusing region as deduced from the backscatter ripples will be different depending upon the side on which the focusing region is assumed to be located. The difference in these magnitudes will become greater as the height above ground of the focusing region becomes smaller. The analysis of the ripples gives no evidence of effects of motions below the $F2$-region.

The analysis of the ripples was done on the assumption that the focusing takes place at reflection layer heights and, since the scatter involved was all $F2$-propagated, this height was taken as 300 km. The comparison of motion characteristics derived on this assumption with motion characteristics found by other workers further served to justify the focusing height chosen.

If the focusing phenomenon occurs at the reflection heights, it is convenient to treat the problem in rather simple terms. Figure 2 is an exaggerated diagram of the backscatter path geometry. The transmitted pulse travels the path from the transmitter, T, to the ionospheric reflection point at M at a height, h, above the ground and then down to the ground at R where it is scattered. Some of the scattered energy retraces the path back to T. The delay time, t, between transmit time and time of scatter return is given by

$$t=\frac{4s}{300} \text{ msec.} \tag{1}$$

where s is in kilometers.

If a focusing region exists at M, there will be an intensification of backscatter amplitude at the corresponding delay time. If the focusing region at M is moving, the delay time of the scatter intensification will increase or decrease depending upon whether the ionospheric great circle distance D, shown in figure 2, is increasing or decreasing.

The relationship between D and delay time, t, is given in figure 3 for a height of 300 km according to the equation

$$D=(r+h)\ \cos^{-1}\frac{r^2+(r+h)^2-(75t)^2}{2r(r+h)}. \tag{2}$$

If D were changing uniformly, and if the units of the abscissa in figure 3 were divided by the rate of change of D, the plot would be one of delay time versus time which is in the form of a backscatter range-time recording. The curve would then represent a ripple changing range on a backscatter range-time recording. In practice, the $F2$-propagated backscatter did not occur at delay times less than 6 or 7 msec for the frequencies used in this experiment so the curve at smaller delays may be disregarded. At greater delays the curve is essentially a straight line.

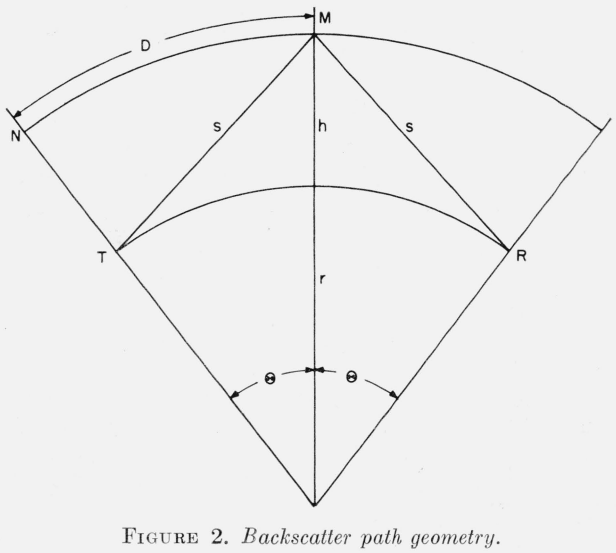

FIGURE 2. *Backscatter path geometry.*

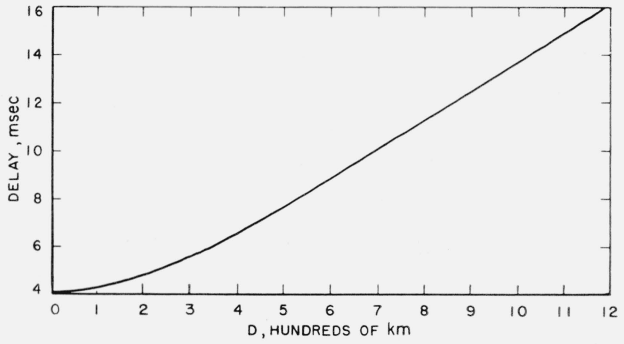

FIGURE 3. *Backscatter delay as a function of the distance, D, of the F layer reflection point.*

Since the speed of the motion is of interest, it is desirable to know the change of D as a function of time, T, for a particular ripple. This is obtained by scaling the slope of the ripple, $\frac{\Delta t}{\Delta T}$, from the range-time recording and multiplying by the reciprocal of the average slope of the delay time versus D curve, $\frac{1}{\frac{\Delta t}{\Delta D}}$, over the delay interval covered by the ripple. As the curve is essentially straight over the range of delay times likely to be encountered, this last quantity may be considered constant and used with all range-time slopes scaled. In other words

$$\frac{\Delta D}{\Delta T}=\frac{\Delta t}{\Delta T}\frac{1}{\frac{\Delta t}{\Delta D}}. \tag{3}$$

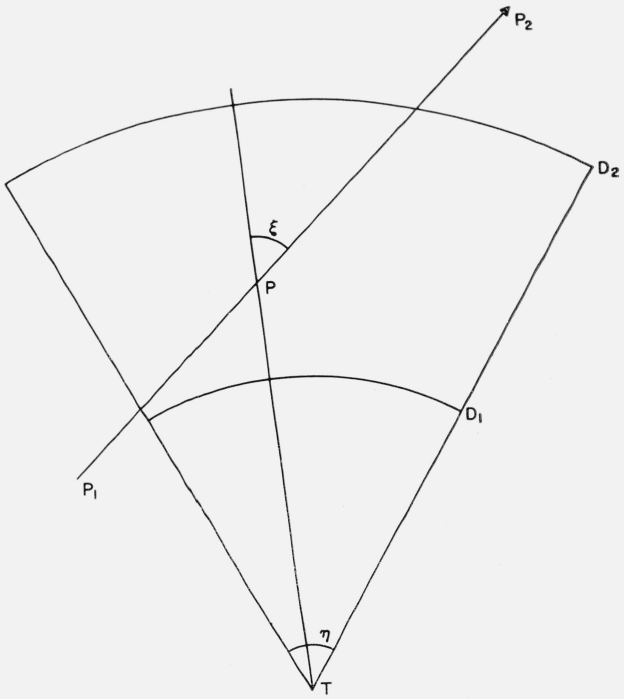

FIGURE 4. *Blob model path geometry.*

If D is in kilometers, T is in hours, and t is delay time in milliseconds, $\frac{\Delta D}{\Delta T}$ is in kilometers per hour. $\frac{1}{\frac{\Delta t}{\Delta D}}$ was calculated at 82.5 km/msec.

This quantity $\frac{\Delta D}{\Delta T}$ represents only the speed of the focusing irregularity toward or away from the transmitting point. Because of the beamwidth of the antenna, it is possible for the irregularity to travel across the beam and the resulting $\frac{\Delta D}{\Delta T}$ scaled would not necessarily be the true speed of the focusing area. How to arrive at the true speed of the focusing area depends upon the model one assumes for this irregularity.

The apparent separations of the focusing irregularities are obtained by scaling the difference in D for two consecutive irregularities on the record at the same time. This is accomplished by measuring the delay time difference in milliseconds at any time and then multiplying by 82.5 km/msec. If two are not visible at the same time, it may be necessary to project the slope of the first one in order to obtain a simultaneous range reading.

The ripples are classified according to whether they represent motions away from the transmitter or motions toward the transmitter. These two groups must be treated separately.

2.3. Focusing Models and Mechanisms

There are two principal models which focusing irregularities may follow. The first is one whose effect is about the same regardless of the azimuth of approach by the sounder pulse. This may be termed the "blob" model as a reflecting blob would exhibit this characteristic. The other may be termed the "long front" model. This would be described as a "wrinkle" in the surface of the reflecting layer extending for a relatively large lateral distance along the front.

In considering the scatter characteristics which these models would provide it is convenient to consider figure 4 in which the area between arcs D_1 and D_2 subtending the antenna beamwidth, η, is the area within which ionospheric reflection and focusing must take place.

a. Blob Model

The blob model will be considered first. In figure 4, let p be a point along the path p_1p_2 followed by a focusing blob moving at a uniform speed, v. The slope of the trace on the backscatter record varies as $v\cos\xi$ as p is allowed to move uniformly along p_1p_2. During the observation time ξ may vary as much as η degrees (in fig. 4 the total variation is about 0.7η). Thus, uniform motion along any straight path through the observation area (except a radial from T) will result in a curved ripple on the backscatter record. For a path crossing the area transversely the ripple will start with a negative slope and end with a positive slope. For radial

paths, cos $\xi=1$, so the slope is constant and equal to v.

There are three kinds of information which can be obtained directly from the scaling of the backscatter ripples. These are the distributions of apparent speeds, the average apparent speed, and the total number of ripples observed per unit time as a function of the antenna azimuth.

If there is an overall preferred direction for the blob motion over the entire area of observation, and further, if there is a certain distribution of the speeds which is the same for all directions of blob motion so that only the number of moving blobs may vary with direction of motion, the above mentioned quantities should vary in the following manner. Without distinguishing between motions toward or away from the transmitter the apparent speed distribution and its average should shift to lower values as the direction of the antenna beam shifts from the preferred direction of blob motion around to 90° and then they should increase again as the beam approaches 180° to the preferred direction.

The number of blobs observed in a given period of time depends upon the size, shape, and orientation of the observation area with respect to the direction of blob travel. For instance, if the distance D_1D_2 in figure 4 were reduced to one-half of that shown, the number of blobs observed moving across the beam would be less than the number observed moving along the beam provided that the blob densities for the two directions of motion were about equal. The motions across the beam would then be discriminated against in the speed distributions. The relative effectiveness of the experimental arrangement for counting blobs moving in a given direction will be designated as the "blob interception cross section" for the given direction. It varies with differing ionospheric conditions and therefore may vary with azimuth.

If the blob interception cross section for any antenna azimuth is approximately constant for all directions of blob travel, the total number of blobs observed per unit time should be about the same at all azimuths. However, if the blobs are separated according to whether their apparent motion is toward or away from the transmitter, then the number having outward motion should be maximum at the antenna azimuth corresponding to the preferred direction. Conversely, the number with inward motion should be maximum at 180° to the preferred direction.

In the actual records, ripples with very low apparent speed were often not scaled because of the difficulty of separating them from other effects. This tends to reduce the total number of blobs counted per unit time and to bias the average apparent speeds toward higher values, particularly for those azimuths at right angles to the preferred direction of blob motion.

If there is sufficient geographical variability in the motion characteristics, some or all of the expected characteristics stated above will be partially or completely masked and any distinguishing features of a particular model may disappear.

b. Long Front Model

The next model to be considered is the long front model. Here the focusing irregularity is considered to lie along a straight line. The motion of this irregularity which may be detected is that perpendicular to its own length. The irregularity is considered to be capable of focusing energy anywhere along its length and regardless of the angle at which the incident beam approaches. This might be difficult to realize in any real case but the concept is useful here.

Figure 5 is similar to figure 4 except that in this case a long front FF′ is moving through the area under observation in the direction of the arrow. Each increment of the front within the beam is focusing some energy. It is seen from the diagram that there would be focused energy returned from nearly minimum scatter range to maximum scatter range, but there is an additional focusing effect due to the concentration in a small increment of delay time of the energy focused by the adjacent elements of the irregularity in the vicinity of p where a radial from T is perpendicular to the front. This concentration should be enough to produce an observable ripple on the scatter record. It is concluded that with this model the ripples appearing on a record for a given antenna azimuth would represent only those irregularities moving along a radial included within the beamwidth, η. The apparent speeds would then be very nearly the actual speeds of the irregularities.

If $n(\theta, v)$ represents the overall density distribution function of the front velocities, then the observed distribution function $N_\theta(v)$ for motions away from the transmitter in a given azimuth, θ, is given by

$$N_\theta(v)=\int_{\theta-\eta/2}^{\theta+\eta/2} n(\theta, v)d\theta. \tag{4}$$

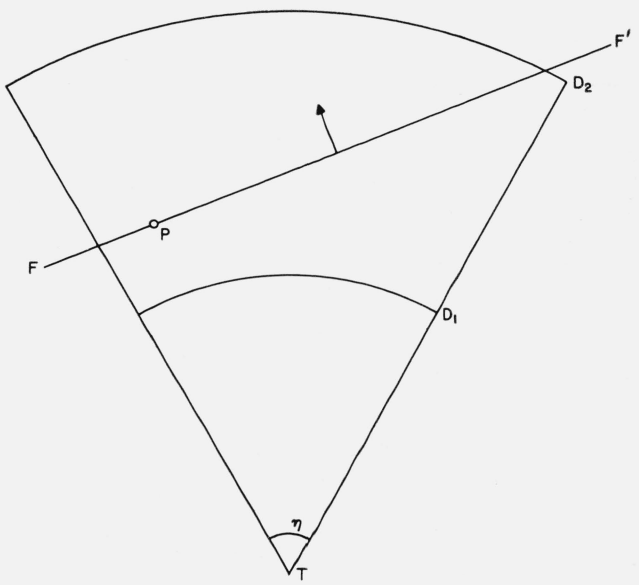

FIGURE 5. *Long front model path geometry.*

$N_{\theta+\pi}(v)$ would be the corresponding distribution for motions toward the transmitter.

If the functional dependence of the distribution on v were the same over the whole geographic area and for all directions (in other words $n(\theta, v)=p(\theta)\ q\ (v)$), this feature should be apparent in the observed distributions for the different antenna azimuths. The average scaled speeds and the normalized speed distributions would be the same for all azimuths. Differences would be indicative of geographic and/or directional variations.

With an overall preferred direction for travel, the number of irregularities moving away from the transmitter should peak as for the blob model at the antenna azimuth corresponding to the preferred direction. Similarly for motions toward the transmitter, there should be a peak at 180° from the preferred direction. Strictly speaking, the converse is not necessarily true. It may not be said with each model that peaks occurring in the manner described definitely imply the existence of an overall preferred direction of travel for the focusing irregularities. However, it seems unlikely that the velocity distributions for different azimuths should be completely different and yet coincidentally provide data as described above.

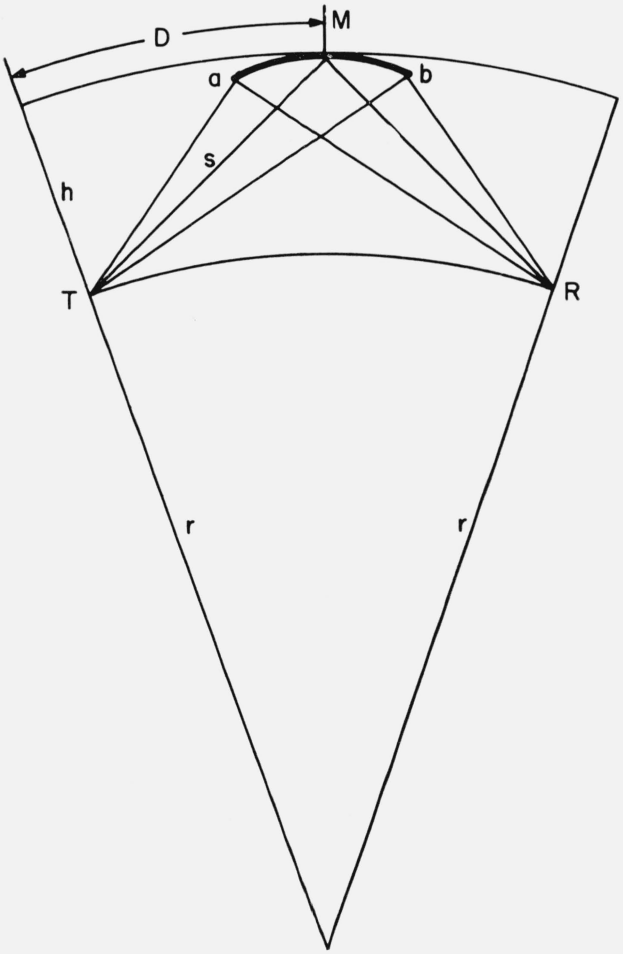

FIGURE 6. *Elliptical focusing mechanism geometry.*

c. Focusing Mechanism

So far nothing has been said regarding the actual focusing mechanism for either the blob or the long front model. A simple mechanism which can be adapted to either model is illustrated in figure 6. Let the element of curved reflecting surface aMb be a part of an ellipse of major axis $2s$ whose focal points are at T and R. Thus, all of the pulse energy radiated into the vertical angle aTb reaches R at exactly the same delay time. The same thing happens to energy scattered over the return path. This energy acts as if it were all transmitted over the path TMR.

It is pertinent to obtain some quantitative information using some of the parameters characteristic of the system used in the experiment. Let the distance ab be 200 km as would be appropriate if the wrinkles were separated by about 400 km. Let $s=900$ km which is a figure near the midrange for most of the scatter observations in this experiment. Let $h=300$ km. The tilt at a or b would then be about 2.5° with respect to the horizontal at the midpoint M, or about 1.7° referred to the horizontal at points a and b. According to Bramley and Ross [1951], such a tilt would not be unusual.

To obtain a simple and fairly adequate blob model one has only to rotate the segment aMb about the line TR. This results in a dimple in the ionospheric surface which will focus energy and behave in general as the blob model. To obtain the long front model one requires the surface generated by moving the segment aMb perpendicular to the plane of the diagram. However, exact adherence to the elliptical model is unnecessary to obtain substantial focusing. Any concave downward surface will give more or less focusing.

The blob type model constructed this way focuses the energy in a roughly circular area about a point on the ground at R. The long front model focuses the energy about a long straight line on the ground. However, as the energy approaches the front at other than perpendicular incidence, the focusing becomes more diffuse about this line as the off perpendicularity increases. This is due to the effectively lateral tilts which operate for obliquely approaching beams. Hence, there is additional reason beyond the clustering of echoes at similar time delays for concluding that backscatter ripples observed with this model include only those fronts moving along a radial included within the antenna beamwidth.

Neither the blob nor the long front mechanism for focusing would be strongly dependent upon frequency. Figure 7, which is a pair of backscatter records made simultaneously on two different backscatter sounders on two different frequencies, indicates by the great similarity in ripple structure that the actual focusing mechanism is not strongly frequency dependent.

These focusing models are not original suggestions since variations of this idea have been used by several workers [Pierce, Mimno, 1940; Munro, 1950; Munro, 1953b; Baird, 1954; Bibl, Harnischmacher, and

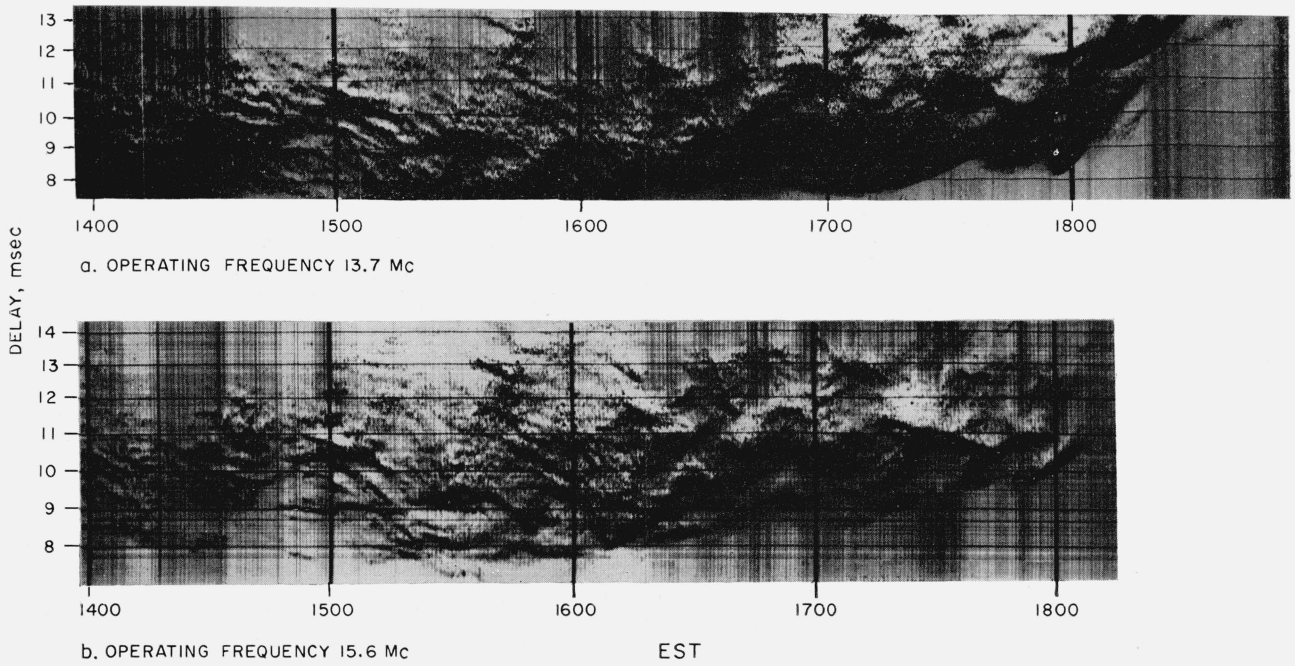

FIGURE 7. *Backscatter records made simultaneously at Sterling, Virginia at azimuth 282°, November 21, 1955.*

Rawer, 1954; Munro and Heisler, 1956a] to explain their observations.

2.4. Experimental Details and Sample Records

The data for the experiment were obtained for the most part from a month's run of the backscatter sounder during December of 1952 at the National Bureau of Standards Field Station at Sterling, Va. The records were made for a different purpose and, consequently, not all of the parameters were ideal for the investigation described here. The records consisted of 16-mm pictures of the backscatter PPI representation described earlier. The transmitter provided pulses of 40 μsec duration and about 500 kw peak power at a repetition rate of 25 pulses per second. The frequency was about 13.7 Mc/s. The antenna was a combination of two vertically polarized three-element Yagis [Silberstein, 1957], and it was rotated continuously at the rate of one rotation per minute.

A T–R network [Hartsfield and Silberstein, 1954] permitted the use of the same antenna for transmitting and receiving. A PPI oscilloscope was electromechanically geared to the antenna such that the oscilloscope trace maintained the same azimuthal bearing as the antenna. A 16-mm motion picture camera was used to photograph the PPI scope face at the rate of one film frame per complete antenna rotation. The result was a series of pictures of the backscatter range and azimuthal characteristics in a precise time sequence.

Figure 8 shows a series of PPI photographs selected at 5 min intervals between 0930 and 1030 EST, December 3, 1952. A little over 30 msec of range are shown on the records with 10 msec separating the intense range markers. The backscatter intensifications are evident here, but the change of range of these intensifications is not at all obvious as it is in the range-time record of figure 1. Any one intensification is evident at quite constant range over a relatively large azimuthal spread. Because of the antenna beamwidth even a small focusing area would be seen over a wide azimuthal range and actually any focusing mechanism will result in the arc-like structure. Thus, motion characteristics are very difficult to obtain using only the PPI pictures directly.

For the scaling of motion characteristics the range-time record mentioned earlier is more convenient. Fortunately, a method of obtaining synthetic range-time records from PPI photographs was available. Briefly, this consisted of using a motion picture projector to project the PPI pictures upon a small translucent slit oriented at the desired azimuth of the PPI image. Viewed from the opposite side from the projector this appeared simply as an intensity modulated trace which could be photographed by a range-time camera in the usual manner. Time marks were made by flashing a light on the slit at intervals determined by a microswitch operated by notches previously cut in the edge of the 16-mm film.

Range-time records for twelve azimuths, 0, 30, 60, 90, 120, 150, 180, 210, 240, 270, 300, and 330 deg were made in this way. Because of the 40° beamwidth between the effective backscatter half-power points, there is some overlap in this arrangement, but it does not materially affect the results. A set of the twelve range-time records for December 3, 1952 is shown in figure 9. A total of about 20 msec or 3000 km of slant range is shown in the records. The base line may appear at ranges somewhat higher than

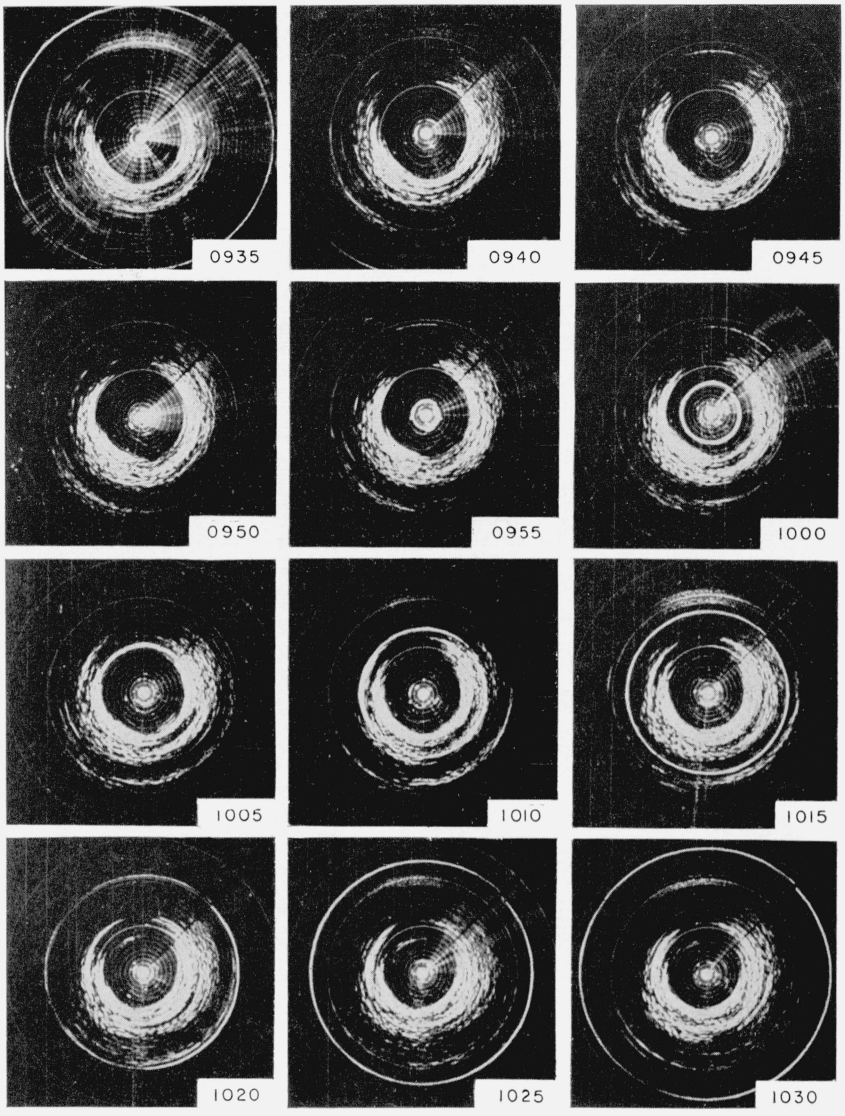

FIGURE 8. *PPI pictures at five minute intervals from 0930–1030 EST, December 3, 1952.*

zero. The time base is not quite uniform from azimuth to azimuth and this had to be taken into account in the scaling procedure. The regular diagonal pattern sweeping from the base line to the top of the record on all azimuths was caused by an interfering pulse from another experiment.

The PPI pictures of figure 8 cover the period between 0930 and 1030 EST on the range-time records in figure 9. The ripples changing in range are very obvious on the range-time recordings whereas, as mentioned earlier, the ripple characteristics are well hidden in the PPI pictures. In some azimuths, notably those around 120°, there seem to be very uniform and regular systems of motion in evidence. The rate of change of range and the separations of the ripples are quite uniform. An interesting feature here is that 180° away, at 300°, there is a regular set of ripples displaying opposite slopes, indicating that the ionospheric motions are in the same general direction in the two regions observed although these regions are separated by over 1500 km.

2.5. Basis for Analysis of Very Large-Scale Disturbances

Ripples in the scatter return are not the only evidence of ionospheric motions in backscatter records. The set of range-time recordings in figure 9 illustrates another evidence of motion. On the 180° azimuth at 1137 EST there is an indentation in the leading edge of the scatter return at about 9 msec delay time. This represents a change in ionization density or reflection height of the ionosphere, in the region where the skip rays are reflected, which causes the skip distance to increase.

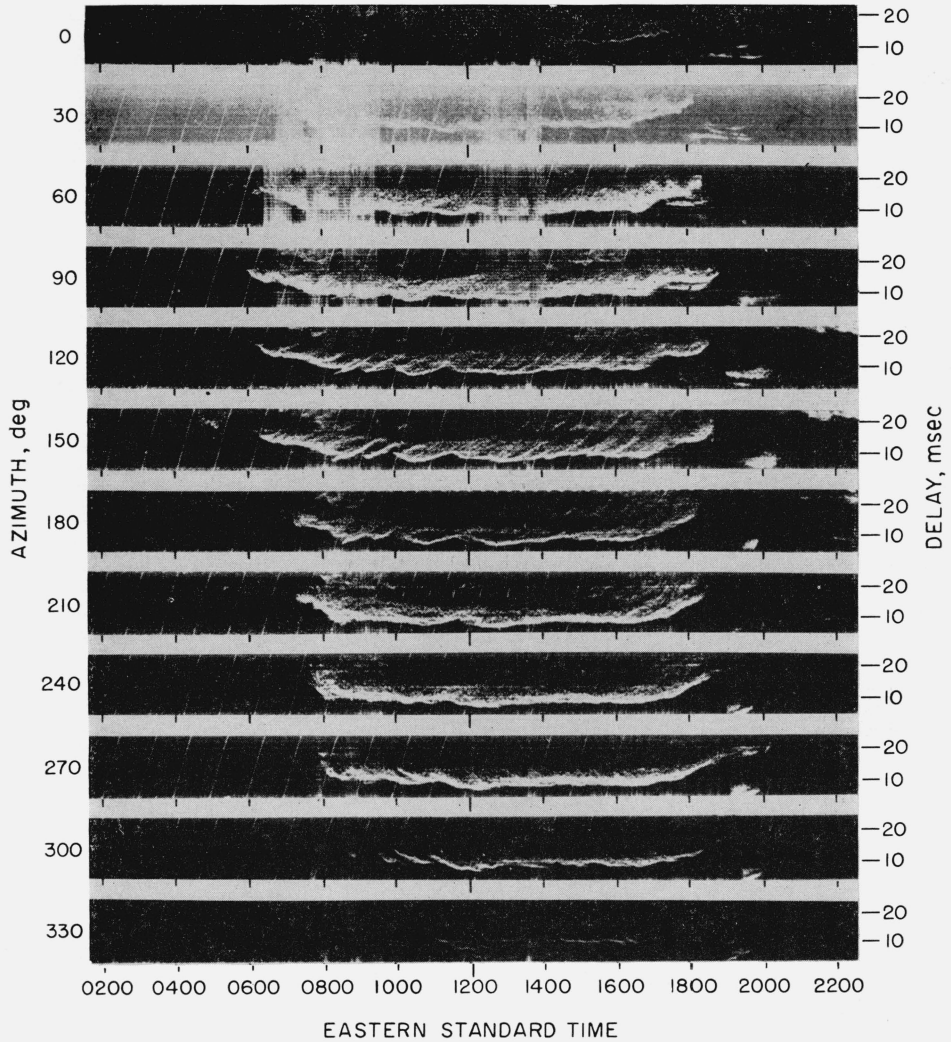

FIGURE 9. *Range-time records for December 3, 1952.*

Indentations are also evident at the neighboring azimuths but at progressively earlier times as the separation from 180° increases in both directions. This situation must be the result of a very large traveling disturbance in the ionosphere. Judging from the widths (durations) of the indentations and the relative time displacements at the different azimuths, this disturbance was about 1500 km across (parallel to the apparent direction of motion) and was traveling from north to south at a speed of about 1500 km/hr. During the thirty days of data several of these disturbances occurred as evidenced by similar patterns of indentations, although the number of azimuths displaying the indentation varied considerably from one disturbance to another. These very large disturbances are probably of the same type as those studied by Valverde [1958] using backscatter PPI pictures and vertical sounders. His measurements indicated some fronts over 4000 km long. The use of range-time records makes the job of analyzing these disturbances perhaps a little easier than the use of the PPI pictures alone.

It should be emphasized that, in contrast to the previously discussed backscatter ripple associated disturbances, of which several may be found in the ionospheric reflection area for the antenna beam at a given time, the very large disturbance is effective over practically the entire beam reflection area at one time. Therefore, the effect of the disturbance is observed regardless of the relationship of the direction of the wave front to the direction of the antenna beam.

A set of range-time records such as in figure 9 involves ionospheric conditions over an annular ring with a minimum radius of about 600 km to a maximum radius of approximately 1200 km about a point above the transmitter as a center. Because of the sequential times of appearance of the indentations at the different azimuths the disturbance appears to be a wide but very long and relatively straight band, and is therefore observed at widely separated geographical points. If the disturbance is nearly symmetrical, the peak of the indentation should indicate the time and range at which the

midline of the disturbance crosses the point whose coordinates are determined from the azimuth and range of the peak of the indentation. Thus, by scaling the time and range of the peak of the indentation for at least three different azimuths, one can obtain a set of geographic locations over which the disturbance passed and the times at which this happened from which one may estimate the magnitude and direction of motion of the disturbance perpendicular to its length.

The problem reduces approximately to one in which a straight wave front passes over points of coordinates X_iY_i in a plane at a time T_i. These quantities are related to the actual problem such that

$$X_i=R_i \cos \theta_i \tag{5}$$

$$Y_i=R_i \sin \theta_i \tag{6}$$

where R_i is obtained from figure 3 and is the value of D corresponding to the delay time to the peak of the indentation on the range-time record and θ_i is the azimuthal bearing at which the range-time record was made. T_i is the time at which the peak of the indentation appeared on the record. Figure 10 illustrates the case.

If the front passes over points 1 and 2 at times T_1 and T_2, the quantity

$$\frac{[(X_1-X_2)^2+(Y_1-Y_2)^2]^{1/2}}{|T_1-T_2|}=v'_{12} \tag{7}$$

is related to the velocity of the front perpendicular to itself by the expression

$$v'_{12}=v \sec (\psi_{12}-\phi) \tag{8}$$

where v is the magnitude of the front velocity, ϕ is its direction, and ψ_{12} is the bearing of point 1 from point 2 when $T_1>T_2$ or the bearing of point 2 from point 1 when $T_2>T_1$. ψ_{12} is obtained from the expression,

$$\tan \psi_{12}=\frac{Y_1-Y_2}{X_1-X_2} \tag{9}$$

when $T_1>T_2$, and from

$$\tan \psi_{12}=\frac{Y_2-Y_1}{X_2-X_1} \tag{10}$$

when $T_2>T_1$. The proper quadrant for ψ_{12} is obtained, of course, by strict observance of the signs of the numerator and the denominator of the equation. Using other points, one obtains other values of v'. If there are N points, there are obtained $\frac{N(N-1)}{2}$ different values of v' each with a particular value of ψ. Having two values of v' and the corresponding ψ's, one may calculate values for v and ϕ by solving two equations of the form of (8) simultaneously. The value of ϕ obtained this way is either the true ϕ or $\phi \pm 180°$. Because of the geometry of the problem the true ϕ may differ from the two ψ's by a maximum of 90° which then makes only one choice possible.

For the present treatment when there were five or more azimuths of observation for a given disturbance, the resulting ten or more values of v' and corresponding ψ were plotted and fitted to a curve of equation (8) by inspection thus yielding the v and the ϕ for the disturbance in question. When there were only three or four observation points, the method of solution by simultaneous equations was used in which every possible set of two values of v' and corresponding ψ's was used to obtain values which were averaged for a final value of v and ϕ.

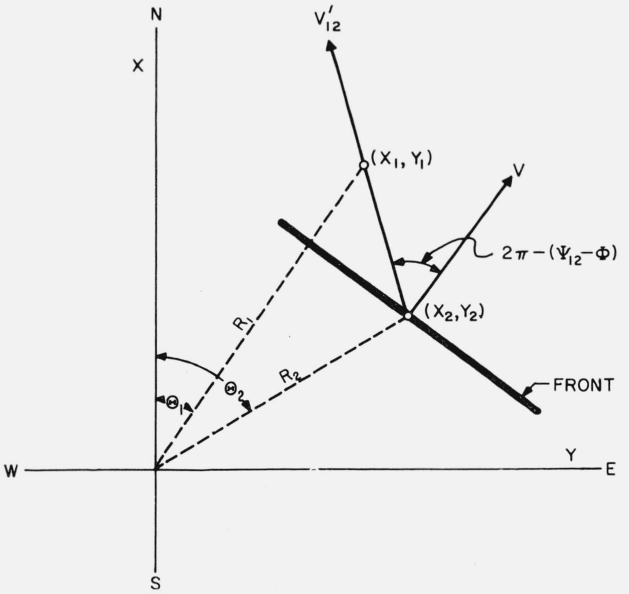

FIGURE 10. *Geometry for very large disturbances.*

3. Results

3.1. Statement of Results

These results are limited in that they were obtained principally during the daylight hours of December 1952. A typical daily set of range-time backscatter records is shown in figure 9. This should be remembered when comparing these results with those of others who have worked at different seasons and different times of day.

Figure 11 is a plot of the average number of ripples per hour of time in which $F2$-propagated ground scatter was evident, for motions away from the transmitter and for motions toward the transmitter, as a function of antenna azimuth. The uncertainty intervals are equal to twice the standard deviation of the mean. The two azimuthal scales are offset by 180° in order to make more obvious the similarity of the two curves.

With either the blob model or the long front model for the focusing irregularities, the distribution shown could result from an approximately uniform directional distribution over the entire area, peaking in

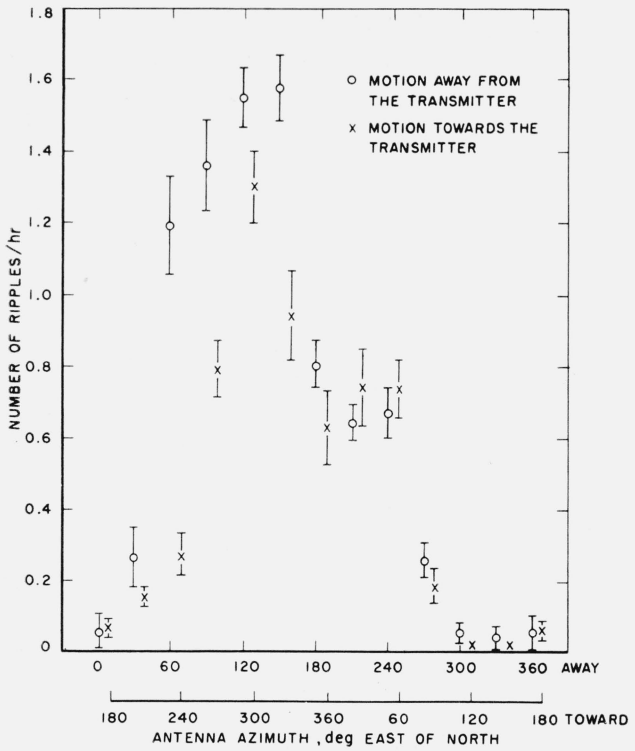

FIGURE 11. *Number of ripples per hour as a function of azimuth.*
Vertical lines extend to plus and minus the standard deviation of the mean.

the southeast direction. Not only do the peaks for motions away from the transmitter occur at azimuths approximately 180° away from those of the motions toward the transmitter, but the minimums behave in the same way, and in each curve the minimum is displaced about 180° from the maximum. The knee in the curve for outward motion at 180° to 240° is very similar to that for inward motion at 0° to 60°. It seems highly unlikely that this pattern should have occurred unless the directional characteristics of the motions were very similar over the entire area involved.

The variations of the mean apparent speed with azimuth, both for motion toward the transmitter and for motion away from the transmitter, are shown in figure 12. The mean apparent speed for motion toward the transmitter is systematically greater than for motion away from the transmitter. The only explanation of this difference that comes to mind is that it resulted from an idiosyncrasy or unconscious bias in the scaling process, but an investigation failed to reveal it. The azimuthal variations, amounting to 30 to 40 percent, have highest values in the northeast quadrant and lowest values in the southwest quadrant.

According to the long front model (section 2.3.b) the observed average speeds would be the same as the true average speeds for the different directions and geographical areas. If the blob model were the correct one, the true average speed would be greater than the average apparent speed since one would observe only the radial component of actual velocity

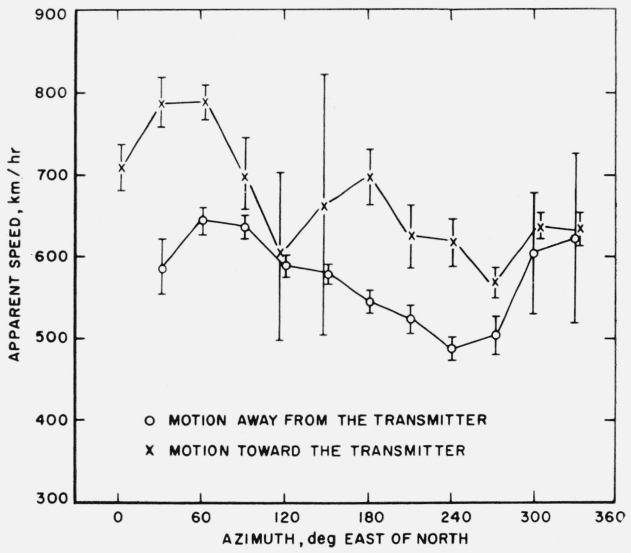

FIGURE 12. *Mean apparent speeds as a function of azimuth.*
Vertical lines extend to plus and minus the standard deviation of the mean. The standard deviation for a single observation varied between 150 and 350 km/hr.

(section 2.3.a), and there would be a tendency for the ratio of apparent to true values to be least in the azimuths at right angles to the preferred direction of motion; i.e., if there were no geographical variations, the average apparent speed would tend to be least in the northeast and southwest quadrants in accordance with the trends of figure 11. Thus the azimuthal variations in figure 12 are not explicable solely in terms of either model, and must be a manifestation of geographical differences in the velocity distribution. As further evidence of geographical differences, the speed distributions for the northeastern azimuths have a much greater proportion of cases in which the speeds fall into the extreme 1200 to 2500 km/hr range. On the other hand, calculations have indicated that the azimuthal variation expected on the basis of the blob model would be small for the directional distribution implied by figure 11, and might be masked by the geographical variations. Thus it must be concluded that these results do not lead to a preference for either the blob model or the long front model for the irregularities.

Figure 13 is a speed distribution histogram showing the number of ripples per 40 km/hr interval for all azimuths taken together. The median value is 580 km/hr.

It should be pointed out that the distribution histogram as plotted in figure 13 and the distributions used to calculate the results in figure 12 are based on the number of irregularities moving through the ionospheric area under observation by the antenna beam in a given period of time. The number observed at any particular speed in a given period must be the actual density of irregularities possessing this speed in the ionosphere multiplied by the product of the speed and the effective cross section for interception of moving irregularities by the antenna beam. The more basic physical quantity is the distribution of the actual number of irregularities per unit area of

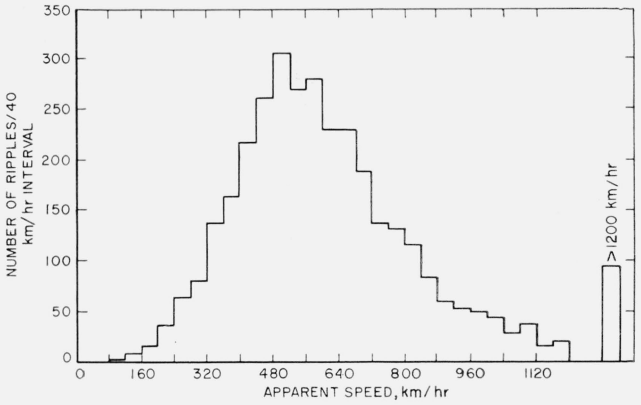

FIGURE 13. *Apparent speed distribution for ripples from all azimuths taken together.*

ionosphere as a function of speed. In the absence of exact knowledge of the interception cross section but assuming it to be constant, one may obtain a relative distribution by taking the distribution histogram as shown in figure 13 and dividing the number per speed interval by the middle speed of the interval. The results given in figure 13 calculated on this basis are given in figure 14. This provides a more symmetrical distribution and provides a new median value of 500 km/hr.

If there were irregularities with no motion or very little motion, they were not detected in scaling the records because of the difficulty in distinguishing them from other effects. Neither type of distribution would then give the proper relationship at very low values of apparent speed.

Range-time records from each azimuth showed relatively brief periods during which the backscatter seemed rather smooth without outstanding irregularities and without evidence of motion. The proportion of time that this occurred during the period of regular $F2$-propagated backscatter averaged about five percent.

No significant difference was found between the speed characteristics of the ripples during the morning when the skip distance was moving into shorter ranges, during the evening when the skip was

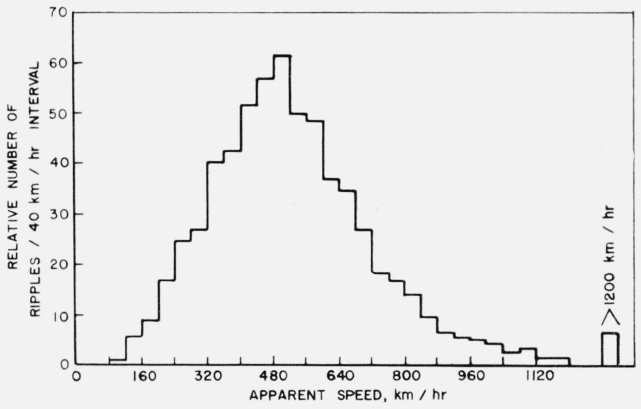

FIGURE 14. *Relative apparent speed distribution corrected to represent the ripple density per unit ionospheric surface area.*

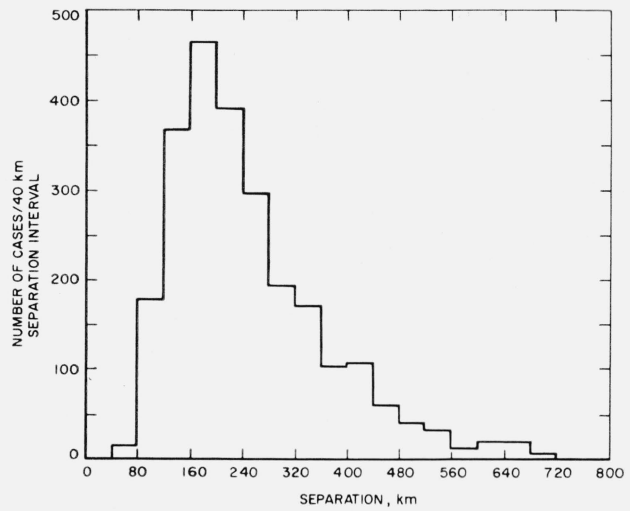

FIGURE 15. *Apparent ripple separation distribution for all azimuths taken together.*

moving out to greater ranges, and during the remainder of the day between these periods when the skip distance was relatively constant.

On a given record, most of the ripples appear in groups and exhibit some differences but seem to be a part of a system. Some appear singly and are separated from their neighbors by relatively large intervals of time and space.

Figure 15 is a distribution histogram giving numbers of separations observed per 40 km interval of separation for all azimuths of observation taken together. Values in the range 160 to 200 km were most frequent. Because of the uncertainties in scaling the separations as they became larger, separations larger than 720 km were not included.

Figure 16 displays the results of the analysis of the very large-scale traveling disturbances. The circles represent the values obtained by fitting the secant curve to the plot of the observed velocity components. The cross marks represent the values obtained by the type of calculation used when there were only three or four azimuths at which the disturbance was recorded.

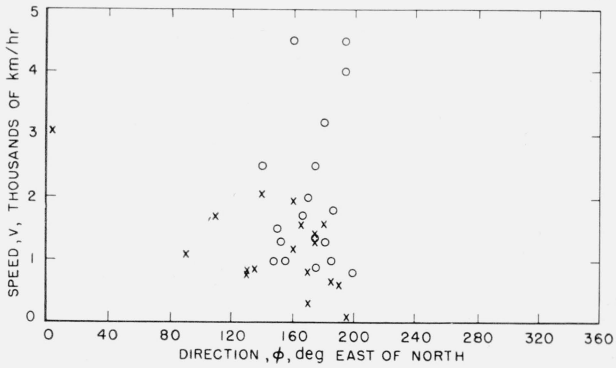

FIGURE 16. *Speed, v, and direction, ϕ, distribution for very large traveling disturbances.*

The majority of these motions of very large disturbances appear between 120° and 200° east of north and have magnitudes of from 100 km/hr to 4500 km/hr. A few larger values were obtained but were omitted because of the large error possible due to the small time increment between azimuthal appearances of the disturbance. Also in these cases the disturbances showed at only three azimuths. The disturbances which appeared at a large number of azimuths vary between 800 km/hr and 4500 km/hr in magnitude. This agrees very well with the results of Valverde at Stanford University for October, November, and December of 1952. His results fall between 750 km/hr and something over 2000 km/hr. It is interesting to note that Valverde's results fall principally between 180° and 225° east of north while those obtained at Sterling, Virginia fall between 120° and 200° east of north. This may indicate an association with the earth's magnetic field.

3.2. Comparison of Results

The results of the backscatter ripple analysis may be summarized by saying that most of the apparent speeds are included in the interval 80–1000 km/hr with a median speed of 580 km/hr or 500 km/hr depending upon whether the distribution is that observed or that calculated from that observed for the population per unit ionospheric area. The overall direction of motion indicated is toward the southeast. The separations between those focusing irregularities which seem to be a part of a system fall between 40 km and 700 km for the most part with the most frequent value at 180 km.

Nearly all of the methods used to measure ionospheric movements in the $F2$-region result in the same range of apparent velocities as obtained in this investigation. Thus the method depending upon the observation of the fading of radio stars at spaced receivers as reported in papers by Maxwell and Little [1952], Maxwell [1954], Maxwell and Dagg [1954] indicates velocities in the high F-region of 100 to 1200 km/hr. The method of similar fades on close spaced receivers as done, for example, by Salzberg and Greenstone [1951], and Chapman [1953] yields values of 250 to 360 km/hr for the F-region. The irregularities utilized with these methods are quite small being of the order of a very few kilometers at the most.

The type of irregularities responsible for backscatter ripples is evidently the same type as those investigated by Munro [1948, 1949, 1950, 1953 a, b], Munro and Heisler [1956 a, b], Price [1954], and McNicol and Webster [1956] in Australia, Beynon [1948], Bramley and Ross [1951], and Bramley [1953] in England, and Pierce and Mimno [1940], and Toman [1955] in the United States. Most of Munro's results indicate a velocity of 300 to 600 km/hr. Price indicates magnitudes of 120 to 1200 km/hr with a most frequent value around 600 km/hr. Beynon obtained a velocity around 430 km/hr and Bramley has found values from 90 to 1300 km/hr with the maximum number of observations about 540 km/hr. Pierce and Mimno derived speeds of 600 to 800 km/hr.

Of particular interest for comparison purposes is the work of Toman [1955] in New England which covered a period including December of 1952. He used a pulse transmitter on fixed frequency and measured the ionospheric movements by observing the relative time delays between the appearances of $F2$ virtual height changes on a system of spaced receivers. Since the distance separating his location from Sterling, Va., is only a few hundred kilometers, it would be expected that the results should be quite similar. He found monthly speed averages ranging from 250 to 600 km/hr with 580 km/hr recorded for December 1952. During the month of December the preferred direction of movement was 117° east of north according to these results. These measurements were made during the daylight hours, and the similarity to the backscatter results is very great.

Munro has reported a generally northeast direction of movements for winter months and a generally southeast direction during the summer with a very fast shift occurring during the period around the equinox. Price has reported a roughly similar result. These are daytime results. Bramley found motion toward the east by day and toward the west at night with a shift at about 1400 u.t. Radio star methods [Maxwell and Little, 1952; Maxwell and Dagg, 1954; and Maxwell, 1954] usable at night indicate a direction toward the west before about midnight and toward the east after that time.

Bramley has reported the wavelengths of the quasi-periodic irregularities in the $F2$-region as varying between 25 and 425 km with a maximum number at 150 km. The vertical amplitude varied up to 4 km. The lateral dimension of one irregularity extended beyond 200 km. Munro and his coworkers in Australia indicated quasi-periodic disturbances with periods of 10 to 60 min and with lateral dimensions perpendicular to the direction of motion exceeding 50 km and some extending to several hundred. These disturbances occur at the rate of one or two per hour with a dimension of 100 to 500 km across a given disturbance. They also point out that the irregularities exhibit a forward tilt with height in the direction of motion with the result that they are noticed first at the higher levels. According to Price the disturbances range from a few to 200 km across and that perpendicular to the direction of travel they exhibit a broad wave front. The number of disturbances observed per hour averaged about 0.4.

McNicol and Webster explained their results in terms of fronts several hundred kilometers long and in the form of a wide inverted trough or in steps with strongly curved edges.

Pierce and Mimno accounted for their results in terms of ionospheric wrinkles of depth less than 5 km and widths of the order of 100 to 500 km.

While the backscatter results did not indicate a preference for either the blob or long front model, some of these other observations point to the possibility that at least a large share of the disturbances are of the long front type.

These are a few results obtained by other workers investigating the problem of ionospheric motions.

A much more complete survey of the subject (up to 1954) is given by Briggs and Spencer [1954].

4. Conclusion

The use of a backscatter sounder appears to be a relatively simple method of determining the direction and apparent speeds of ionospheric motions when these characteristics are fairly uniform over the relatively large area observed by the sounder. Even in the absence of uniformity useful information about the magnitudes of apparent speeds is still available from a single sounder. It has been shown that the results obtained using the backscatter sounder are in good agreement with those obtained using other methods.

Future experimentation should be directed toward determining the form and focusing characteristics of the ionospheric irregularities themselves. The use of variable pulse lengths, different antenna beams, and concerted action by several sounders of both the vertical and backscatter type should yield considerable information about these irregularities.

The author expresses his appreciation to Richard Silberstein, who suggested the investigation, for his continuing interest and suggestions, to William Hartsfield who devised the method for making synthetic range-time recordings and under whose project leadership the backscatter run was made, and to Thomas Gautier for the many helpful suggestions and valuable discussions.

5. References

Baird, K., High multiple radio reflections from the F–2 layer of the ionosphere at Brisbane, Australian J. Phys. **7,** No. 1, 165–175 (Mar. 1954).

Bibl, K., E. Harnischmacher, and K. Rawer, Some observations of ionospheric movements, Report of the Physical Society Conference on Physics of the Ionosphere, London, 113–118 (Sept. 1954).

Beynon, W.J.G., Evidence of horizontal motion in region F–2 ionization, Nature **162,** 887 (Dec. 4, 1948).

Bramley, E. N., Direction finding studies of large scale ionospheric irregularities, Proc. Roy. Soc. [A] **220,** 39–61 (Oct. 22, 1953).

Bramley, E. N., and W. Ross, Measurements of the direction of arrival of short radio waves reflected at the ionosphere, Proc. Roy. Soc. [A] **207,** 251–267 (June 22, 1951).

Briggs, B. H., and M. Spencer, Horizontal movements in the ionosphere, Reports on Progress in Physics **17,** No. 254, 245–280 (1954).

Chapman, J. H., A study of winds in the ionosphere by radio methods, Can. J. Phys. **31,** No. 1, 120–131 (Jan. 1953).

Clark, C., and A. M. Peterson, Motion of sporadic-E patches determined from high-frequency backscatter records, Nature **178,** 486–487 (Sept. 1, 1956).

Dieminger, W., The scattering of radio waves, Proc. Phys. Soc. **64,** No. 2, 142–158 (Feb. 1951).

Gerson, N. C., Large scale sporadic movements of the D-layer of the ionosphere, Nature **166,** 316–317 (Aug. 19, 1950).

Hartsfield, W. L., S. M. Ostrow, and R. Silberstein, Backscatter observations by the Central Radio Propagation Laboratory—August 1947 to March 1948, J. Research NBS **44,** 199–214 (Feb. 1950).

Hartsfield, W. L., and R. Silberstein, A comparison of C–W field intensity and backscatter delay, Proc. IRE **40,** No. 12, 1700–1706 (Dec. 1952).

Hartsfield, W. L., and R. Silberstein, Low-pass duplexing system for high-frequency pulse transmitters, Tele-Tech **13,** No. 2, 76 (Feb. 1954).

Manning, L. A., O. G. Villard, and A. M. Peterson, Meteoric echo study of upper atmosphere winds, Proc. IRE **38,** No. 8, 877–883 (Aug. 1950).

Maxwell, A., Investigation of F region drift movements by observations of radio star fading, Report of the Physical Society Conference on Physics of the Ionosphere, London, 166–171 (Sept. 1954).

Maxwell, A., and M. Dagg, A radio astronomical investigation of drift movements in the upper atmosphere, Phil. Mag. [7] **45,** 551–569 (June 1954).

Maxwell, A., and C. G. Little, A radio-astronomical investigation of winds in the upper atmosphere, Nature **169,** 746–747 (May 3, 1952).

McNicol, R. W. E., and H. C. Webster, A study of "Spread-F" ionospheric echoes at night at Brisbane, II. Interpretation of range spreading, Australian J. Phys. **9,** No. 2, 272–285 (June 1956).

Meek, J. H., Sporadic ionization at high latitudes, J. Geophys. Research **54,** No. 3, 284–285 (Sept. 1949).

Mitra, S. N., A radio method of measuring winds in the ionosphere, Proc. Inst. Elec. Engrs. **96,** Part III, No. 43, 441–446 (Sept. 1949).

Munro, G. H., Short period changes in the F region of the ionosphere, Nature **162,** 886–887 (Dec. 4, 1948).

Munro, G. H., Short-period variations in the ionosphere, Nature **163,** 812–814 (May 21, 1949).

Munro, G. H., Traveling disturbances in the ionosphere, Proc. Roy. Soc. [A] **202,** 208–223 (July 7, 1950).

Munro, G. H., Traveling disturbances in the ionosphere: Diurnal variation of direction, Nature **171,** 693–694 (April 18, 1953a).

Munro, G. H., Reflexions from irregularities in the ionosphere, Proc. Roy. Soc. [A] **219,** 447–463 (Oct. 1953b).

Munro, G. H., and L. H. Heisler, Cusp type anomalies in variable frequency ionospheric records, Australian J. Phys. **9,** No. 3, 343–358 (Sept. 1956a).

Munro, G. H., and L. H. Heisler, Divergence of radio rays in the ionosphere, Australian J. Phys. **9,** No. 3, 359–372 (Sept. 1956b).

Peterson, A. M., The mechanism of F-layer propagated backscatter echoes, J. Geophys. Research **56,** No. 2, 221–237 (June 1951).

Pierce, J. A., and H. R. Mimno, The reception of radio echoes from distant ionospheric irregularities, Phys. Rev. **57,** No. 2, 95–105 (Jan. 15, 1940).

Price, R. E., Traveling disturbances in the ionosphere, Report of the Physical Society Conference on Physics of the Ionosphere, London, 181–190 (Sept. 1954).

Salzberg, C. D., and R. Greenstone, Systematic ionospheric winds, J. Geophys. Research **56,** No. 4, 521–533 (Dec. 1951).

Shearman, E. D. R., The technique of ionospheric investigation using ground backscatter, Proc. Inst. Elec. Engrs. **103,** pt. B, No. 8, 210–223 (March 1956).

Silberstein, R., High frequency scatter sounding experiments at the National Bureau of Standards, Science **118,** 759–763 (December 25, 1953).

Silberstein, R., The long-distance horizontal radiation pattern of a high-frequency antenna, IRE Tran. on Antennas and Propagation **AP–5,** No. 4, p. 397 (Oct. 1957).

Toman, K., Movement of the F region, J. Geophys. Research **60,** No. 1, 57–70 (March 1955).

Valverde, J. F., Motions of large-scale traveling disturbances determined from high-frequency backscatter and vertical incidence records, Radio Propagation Laboratory, Stanford Univ. Sci. Rept. No. 1 (May 21, 1958).

Wells, H. W., Large-scale movements of the layers,Proceedings of Polar Atmosphere Symposium, Part 2: Ionospheric Section, (Pergamon Press, 1957). (Also published as a special supplement to the J. Atmospheric and Terrest. Phys., 33–40, 1957.)

(Paper 65D2–109)